# Effect of mixed-phase cloud on the chemical budget of trace gases: A modeling approach

Yoann Long, Nadine Chaumerliac, Laurent Deguillaume, Maud Leriche, François Champeau

# "Effect of mixed-phase cloud on the chemical budget of trace gases: a modeling approach"

Y. Long[1,2], N. Chaumerliac[1,2], L. Deguillaume[1,2], M. Leriche[3], F. Champeau[1,2]

[1] Clermont Université, Université Blaise Pascal, LaMP, BP 10448, F-63000 CLERMONT-FERRAND

[2] CNRS, UMR 6016, LaMP, F-63177 AUBIERE

[3] Laboratoire d'Aérologie, CNRS, 14 avenue Edouard Belin, F-31400 TOULOUSE

Submitted to **Atmospheric Research**

Corresponding author:

Nadine Chaumerliac
LaMP
N.Chaumerliac@opgc.univ-bpclermont.fr

## Abstract

A multiphase cloud chemistry model coupling a detailed chemical reactivity mechanism in gas phase and aqueous phase to a cloud parcel model with a two-moment microphysical scheme has been extended to include ice phase processes. This newly developed model is used to study the influence of the ice phase on HCOOH, $HNO_3$, $H_2O_2$ and $CH_2O$ in a mixed-phase cloud. Microphysical processes are describing the interactions between the water vapor phase, the liquid phase (cloud and rain water) and the ice phase (pristine ice, snow and graupel) in the cloud and for soluble chemical species, their transfer by mixed-phase microphysical processes has been included. In addition to microphysical transfer between iced hydrometeors, the probable two main processes incorporating soluble chemical species in iced hydrometeors are the retention in ice phase as riming or freezing occurs and the burial in the ice crystal as the crystal grows by vapor diffusion.

The model is applied to a cloud event describing a moderate precipitating mixed-phase cloud forming in a continental air mass in winter. The main features of the cloud are described and the evolution of key chemical species as function of time and temperature is discussed. Sensitivity tests are performed: a run without ice to highlight the influence of ice phase on the chemical gas phase composition of the cloud, a run without burial showing that it is a negligible process, a run assuming full retention in ice for all species and a run varying the ice crystal shapes. A detailed analysis of the microphysical rates and chemical rates linked to retention and burial effects show that for this cloud event, the effect of the ice phase on gas phase composition is driven by riming of cloud droplets onto graupels, which leads to retention or not of soluble chemical species in the ice phase. Finally, the impact of crystal geometry on the efficiency of collection is studied together with its impact on the riming of cloud droplets on graupels and also on the retention of chemical species in ice phase.

**Keywords:** multiphase chemistry, cloud modeling, mixed-phase microphysics.

# 1. INTRODUCTION

Clouds, which cover 50% of terrestrial surface, influence the redistribution of traces gases between the different layers of atmosphere and modify the Earth's radiative budget. Among those, mixed-phase convective clouds constitute 60 % of all clouds (Hegg, 2001). As ice develops in clouds, it influences all major cloud characteristics including precipitation formation (Tao, 2003), interactions with radiation (Ackerman et al., 1998; Liu et al., 2003), latent heat release and cloud dynamics (Willoughby et al., 1985), and water vapor content (Heymsfield et al., 1998).

The presence of ice favors tracer vertical transport due to intensified latent heat effects, modifies the exchange of matter among the various water phases, and perturbs photochemistry through retroaction between ice and radiation and reactivity pathways. Also, the terminal fall speed of the solid hydrometeors is significantly reduced compared to that of the liquid drops of the same weight. A possible consequence of these different aerodynamical properties is that partially glaciated clouds can be expected to provide a larger residence time of solid hydrometeors that can favor gas and aerosol scavenging (Lawrence and Crutzen, 1998).

Due to the variety of effects of clouds on tropospheric chemistry, there have been considerable efforts to understand the complex processes of clouds through in-situ measurements, laboratory experiments and modeling studies. These have included numerous studies focused on the effects of ice clouds on dynamics and precipitation (Rutledge and Hobbs, 1984; Reisner et al., 1998; Thompson et al., 2006). There have been also many studies on gaseous tracer cloud venting (Flossmann and Wobrock, 1996; Cotton et al., 1995; Yin et al., 2002) and of cloud chemistry pertinent to specific impacts such as acidic precipitation (Barth et al., 2002; Leriche et al., 2007).

One area of cloud chemical processing that is still not well understood involves interactions of ice-phase cloud hydrometeors with chemical species. There are various iced hydrometeors (pristine, snow, graupel…) with a large range of sizes, shapes and characteristics like the level of riming for instance. Ice-chemical interactions include gas-ice transfer, partitioning during freezing of liquid hydrometeors, surface and bulk reactions in/on ice hydrometeors. Experimental studies have shown that the amount of gas taken up by an ice surface is dependent on the type of gas, the temperature, the crystalline structure of the ice and on whether the uptake takes place on a growing or non-growing ice surface (Pruppacher and Klett, 1997; Huthwelker et al., 2006), which is the relevant atmospheric case. The recent paper from Kärcher et al. (2009) presents a theoretical approach of the uptake of gases by ice crystals, which considers the combined effect of mass accommodation and net adsorption of trace gases on the surfaces of growing ice particles. However, this approach is limited to nitric acid and is not directly applicable to other species. An alternative approach is to use a single parameter, the burial coefficient that describes different efficiencies of gas trapping in growing ice hydrometeors (Yin et al., 2002). The partitioning of soluble gases during the freezing of liquid hydrometeors is classically obtained by a retention coefficient describing the fraction of a dissolved trace gas which is retained in hydrometeors during freezing. The information is almost non-existent for the surface of bulk reactivity of chemical species in the ice crystals and concerns mainly stratospheric conditions (Sander et al., 2006).

Previous modeling studies that have included some interactions between volatile chemicals and ice phase particles have found that they may significantly impact chemical distributions and deposition (Rutledge et al., 1986; Chen and Lamb, 1990; Wang and Chang, 1993; Audiffren et al., 1998; Barth et al., 2001; Yin et al., 2002; Salzmann et al., 2007). Simulated impacts have included enhanced scavenging of intermediate to highly soluble species (Barth et al., 2001), higher amounts of $H_2O_2$ and sulphates in precipitation (Audiffren et al., 1999),

suppression of $H_2O_2$ scavenging in the glaciated part of the cloud that might explain the observations of enhanced $H_2O_2$ in outflow from tropical deep convection (Mari et al., 2000; Salzmann et al., 2007). Modelling results also suggest that the parameterization of partitioning can strongly affect the simulated outcome (Chen and Lamb, 1990 ; Barth et al., 2001), though results may also depend on the cloud type (Yin et al., 2002) and the convection initiation representation (Salzmann et al., 2007). However, most of them limit their studies to soluble tracers assuming Henry's law equilibrium and did not discuss in details solubility, retention coefficients and uptake efficiencies onto ice particles for gases described with explicit chemistry fully coupled with microphysics. They mainly focused on cloud vertical transport of species rather than studying in details the partitioning of species among gas, liquid and solid phases by microphysical processes.

In this paper, we investigate the role of ice-phase processes on chemistry in the case of an isolated cloud, even if cloud dynamics is not fully represented. Exchanges of chemical species between gas phase, cloud droplets, raindrops and ice particles are studied in details with considering three ice categories (pristine, snow and graupel) distributed with a gamma function. The study is based upon a 1D model with entrainment coupling two-moment microphysics derived from Thompson et al. (2004) with an explicit multiphase chemistry model (Leriche et al., 2000; 2007).

In the first part of this paper, the microphysical scheme extension to ice phase is briefly described since it is based upon the works of Thompson et al. (2004) and Morrison and Grabowski (2008). Then, results are presented from a simulation case derived from Audiffren et al. (1998) that considered very limited chemistry compared to the one presented in this paper. Indeed, for this modeling study, the chemistry includes 282 reactions with 180 reactions in the aqueous phase, 102 reactions in the gas phase and 54 mass transfer exchanges between gas and aqueous phases and fully coupled scavenging processes. Results are

presented pertaining to the partitioning of soluble gas phase compounds among the various phases and discuss the potential importance of mixed-phase processes compared to only warm ones. Finally, sensitivity tests address the question of the influence of crystal shape on gas scavenging by mixed-phase microphysical processes.

# 2. MODEL FORMULATION

## 2.1. Description of the M2C2 model

The Model of Multiphase Cloud Chemistry (M2C2) has been developed to simulate tropospheric cloud events and results from the coupling (Leriche et al., 2001) between a multiphase chemistry model with explicit multiphase chemical mechanisms (Leriche et al., 2000, 2003; Deguillaume et al., 2004) and a two moment microphysical scheme (Caro et al., 2004). Initially, the dynamical framework of this model was an air parcel (Gérémy et al., 2000) that has been recently improved with entrainment/detrainment processes.

The chemistry included in the chemical module is explicit and describes the exchanges of chemical species between the gas phase and the aqueous phase, which is parameterized following the mass transfer kinetic formulation developed by Schwartz (1986). In the full mechanism, the aqueous phase chemistry includes the detailed chemistry of $H_xO_y$ , chlorine, carbonates, $NO_y$ , sulfur, the oxidation of organic volatile compounds (VOCs) with two carbon atom (Leriche et al., 2003; 2007), the chemistry of transition metal ions for iron, manganese and copper (Deguillaume et al., 2004; 2005). Aerosol particles temporal evolution and their activation in cloud droplets can also be described using the parameterization of droplets nucleation from Abdul-Razzak and Ghan (2000) since aerosol particles contribute to the chemical composition of cloud droplets by nucleation and impaction scavenging followed by dissolution of soluble compounds (Leriche et al., 2007). The model considers calculations

of photolysis frequencies both in the gas phase and in cloud droplets. The pH is calculated at each time step by solving the electroneutrality equation.

However, in the atmospheric environment cloud evolution and scavenging of gases and aerosol particles are also modified by the presence of ice phase (Willoughby et al., 1985; Michael and Stuart, 2009). Special attention is given in the next sections to the extension of the actual microphysical scheme to ice phase and mixed-phase processes, based on the approach of Thompson et al. (2004).

## 2.2. Description of the warm microphysical module

First, the "warm" microphysical module presented in detail in Leriche et al. (2001) and Leriche et al. (2007) is briefly recalled here. The microphysical module derives from the parameterization of Chaumerliac et al. (1987) that considers two liquid water categories (cloud water and rain) distributed according to log-normal distributions, $G(D)$:

$$G(D) = \frac{1}{\sqrt{2\pi\sigma D}} \exp\left( -\frac{1}{2\sigma^2} \ln^2\left( \frac{D}{D_0} \right) \right) \quad (1)$$

*D: geometric diameter; $D_0$ : median geometric diameter; $\sigma$ : geometric standard deviation.*

The considered microphysical processes are droplet nucleation, condensation / evaporation, collision / coalescence and sedimentation (Berry and Reinhardt, 1974a, b, c, d). Cloud water and rainwater number concentration and mixing ratios are calculated in a prognostic way at each microphysical time step ($\Delta t$ = 5s).

Nucleation processes are parameterized following Chaumerliac et al. (1987) who uses an activation spectrum to form cloud droplets:

$$N = CS^k \quad (2)$$

*where S is the supersaturation and C and k empirical constants related to the origin of the air mass (moderate continental in this paper, with C=600 $cm^{-3}$ and k=0.7).*

## 2.3. New developments – mixed-phase cloud microphysics

This part of the manuscript describes the recent developments of the M2C2 model for simulating mixed-phase clouds with a two-moment scheme. The introduction of these new processes in the model are going first to feedback on the temperature through latent heat release effects which can be expressed with the net latent heat release rate (LHR) through phase changes among different cloud species as:

$$LHR = Lv\,[CONDQCW + CONDQRW - EVAPMQS - EVAPMQG] + Ls\,[XNUCQI(T<T_0) + DEPVQI(T<T_0) + DEPQSNOW(T<T_0) + DEPQGRAUP(T<T_0)] + Lf\,[FREZQR(T_{00}<T<T_0)] + FREZQI(T_{00}<T<T_0) + RIMQI(T<T_0) + COLLQCS(T<T_0) + COLLQRIG(T<T_0) + COLLQCG(T<T_0) + COLLQRS(T<T_0) + COLLQRG(T<T_0) - XMELTQS(T>T_0) - XMELTRG(T>T_0) - XMELTCG(T>T_0) - XMELTQG(T>T_0)] \quad (3)$$

*where Lv, Ls, and Lf are latent heat of vaporization, sublimation, and fusion (J/kg) at $T_0$=0°C, respectively, Ls=Lv+Lf; $T_{00}$=-35°C; LHR is the net latent heat release rate (J/kg/s).*

The various microphysical rates involved in the calculation of net latent heat release term are reported in the list of symbols at the end of the manuscript and in the scheme in Figure 1 which summarizes the mixed-phase microphysics, considered in the M2C2 model. Mixed-phase processes include pristine formation, vapor deposition and collision / coalescence growth, evaporation, sedimentation and complex conversions between hydrometeors categories, such as aggregation, accretion, riming, freezing, melting and sublimation.

The introduction of the ice phase implies interactions between ice crystals and raindrops which will be easier to represent if both kind of hydrometeors are distributed with a similar distribution function; therefore, a generalized gamma distribution (Meyers et al., 1997) is used with the consideration of the shape parameter, $\nu$ :

$$G(D) = \frac{\alpha}{\Gamma(\nu)} \frac{1}{D_n} \left( \frac{D}{D_n} \right)^{\alpha\nu - 1} \exp\left[ - \left( \frac{D}{D_n} \right)^{\alpha} \right] \quad (4)$$

*where $D_n$ is the mean diameter of the distribution; $\nu$ and $\alpha$ are parameters which allow to adjust the distribution shape; $\Gamma(\nu)$ is the gamma function.*

A log-normal distribution is maintained for cloud water resulting only from aerosol activation and melting of ice crystals.

The mixed-phase scheme predicts the evolution of six water species: $q_v$ (vapor), $q_{cw}$ and $q_{rw}$ (cloud droplets and raindrops) and $q_{ice}$, $q_{snow}$ and $q_{graup}$ (pristine ice, snow and graupel defined by an increasing degree of riming) for the mixing ratios and $N_{cw}$, $N_{rw}$ for the total number concentrations of cloud droplets and raindrops respectively and $N_{ice}$, $N_{snow}$ and $N_{graup}$ for the total number concentrations of pristine ice, snow and graupel respectively. The use of two classes of liquid hydrometeors together with three classes of iced hydrometeors is required to properly represent ice phase in mixed-phase clouds (Mc Cumber et al., 1991).

The mixed-phase scheme used in this study corresponds to the updated version of the Reisner's scheme by Thompson et al. (2004), for the prediction of mixing ratios for ice pristine, snow and graupel. Ice number concentrations are a total of three prognostic variables described in the scheme of Morrison and Grabowski (2008) and the reader is referred to these publications for further details.

The pristine ice category is initiated by homogeneous nucleation when the temperature is less than -35°C or more likely by heterogeneous nucleation and the number of ice crystals newly formed follow the Cooper's (1986) empirical parameterization based on direct ice crystal measurements.

Ice crystal multiplication in the model can increase the crystal concentration through rime splintering (Hallet and Mossop, 1974). However, this case study mostly lies outside the assumed temperature range for rime splintering to occur. These crystals grow by water vapor

deposition and/or at the expense of cloud droplets by the Bergeron-Findeisen effect. The snow phase is initiated by autoconversion of the primary crystals; it grows by deposition of water, by aggregation through small crystals collection and by the light riming produced by impaction of cloud droplets and of raindrops. Graupels are produced by the heavy riming of snow and by rain freezing when supercooled raindrops get in contact with pristine ice crystals.

According to the heat balance equation and to the efficiency of their collecting capacity, graupels can grow either in the dry mode or in the wet mode when riming is very intense (as for hailstone embryos). In the latter case, the excess of non-freezable liquid water at the surface of the graupels is shed and evacuated to form raindrops. When the temperature becomes positive, pristine crystals immediately melt into cloud droplets, while snowflakes are progressively converted into graupels that melt as they fall.

Furthermore, the scheme also predicts number concentration as in Morrison and Grabowski (2008); processes that involve particle concentration change have to be considered. The change in snow and graupel number concentration due to melting and sublimation is calculated by assuming that the relative change in number concentration is the same as the change in mixing ratio due to these processes following Ferrier (1994). It is also assumed that the decrease of number concentration during sublimation of snow and graupel is the same as mixing ratio, which implies that the mean size does not change. The increase in rain number concentration due to melting is equal to the decrease of graupel and snow number concentration. In the case of evaporation/sublimation shrinking, the number is only adjusted upon complete evaporation/sublimation.

Size and fall velocity of the various hydrometeors are provided in Table 1 since they determine the collection and the growth of the various ice categories thereby influencing the partitioning of gases among them as detailed later on in section 4.

Two cases are considered, depending on whether snow and graupel are spherical particles or not. We assume that main differences are for snow and graupel categories. For snow, we chose 2D plate cold-type particles (Woods et al., 2007), which are typical at temperature range from -8°C to -12°C and non-spherical for graupel. Crystal shape influences the fall velocity which determines the residence time of hydrometeors during which they can scavenge chemicals. Also, in the two cases, we can expect different levels of riming that will perturb gas scavenging.

## 2.4. New developments: gas scavenging by ice hydrometeors

The effects of clouds on chemistry through microphysical processes are treated as transfer rates of the gases dissolved in cloud droplets or raindrops that are proportional to the microphysical rates of autoconversion, accretion and sedimentation. Gases dissolved and scavenged by the liquid hydrometeors after mass transfer are released back to the gas phase in case of evaporation. Same treatment is applied for gases attached to the ice-phase hydrometeors and exchanges between pristine, snow and graupel follow the microphysical processes describing the autoconversion, the aggregation and collection of crystals among the three ice categories. Concerning microphysical processes between liquid and ice or between vapor and ice, a different treatment is applied for the volatile chemical phase partitioning during freezing and riming and also during the growth of ice crystals by vapor diffusion respectively.

During riming and freezing, only a fraction of the gas $R_c$ is retained by the ice crystal and $(1-R_c)$ is released to the gas phase (Yin et al., 2002).

Given the uncertainties in the physical processes driving gas uptake by ice crystals, the growth of ice by diffusion of water vapor is assumed to lead to the burial of the trace gas molecules following Yin et al. (2002). One gas molecule that becomes attached to the surface

of a growing crystal rapidly becomes entrapped under several layers of ice before they have a chance to desorb. To represent such a process, a burial efficiency $\beta$ is defined with a value of 1 if all the trace gas molecules that diffuse on the growing crystal surface become buried, while a smaller value of $\beta$ implies that a weak interaction with the ice surface so that gases are not efficiently captured in the ice crystal.

The main limitation for describing retention ($R_c$) and burial ($\beta$) is that they are poorly known even if several laboratory and experimental studies have studied phase partitioning during the liquid-to-solid freezing and riming (Iribarne and Pyshnov, 1990a,b; Lamb and Blumenstein, 1987; Snider et al., 1992; Voisin et al., 2000). Some values of the retention coefficient $R_c$ are available in the literature for species such as $SO_2$, $H_2O_2$, HCHO, $HNO_3$, HCOOH and are reported in Figure 2. The most common formulation for the retention coefficient is the one from Lamb and Blumenstein (1987):

$$\mathrm{RET} = 0.012 + 0.0058\left(\mathrm{T} - \mathrm{T}_0\right) \tag{5}$$

which has been adopted for almost all species, like for instance HCOOH. Exceptions are for $H_2O_2$, $CH_3OOH$, $SO_2$ and $CH_2O$, $HNO_3$, HCl. A value of 0.5 is taken for $H_2O_2$ (Snider et al., 1992), a value of 0.02 is taken for $CH_2O$, $CH_3OOH$ (Mari et al., 2000) and for $SO_2$ (Voisin et al., 2000), and a value of 1 is applied for strong acids: nitric, sulfuric and chloridric acid (Iribarne and Pyshnov, 1990a).

Figure 2 shows the retention coefficient of several species as a function of their effective Henry's law constant (see Sander, 1999) for a range of temperatures between -20°C and 0°C. This figure illustrates the contrasted behavior for a panel of gases more or less soluble and more or less sensitive to uptake in ice phase. These values and variations of both retention coefficients and Henry's law constant will help us in interpreting further results in the next sections. For instance, nitric acid is very soluble and has a retention coefficient of 1.

However no single factor controls the extremes of the retention coefficient which varies between 0 and 1, rather combination of factors such as solubility, but also ice-liquid interface supercooling, wet or dry growth conditions, as discussed by Michael and Stuart (2009).

The situation is even worse for the burial coefficient which has never been documented. In this paper, the burial coefficient is set constant, equal to 1, which means that the gas is retained in the crystal when it growths by vapor diffusion.

In the model, the processes of burial and retention are represented as transfer between two phases and are written with proportionality relationships.

So in the gas phase, during riming and freezing processes, the retention coefficient *RET* is used to calculate the concentration change rates as follows:

$$\left(\frac{\partial C_g}{\partial t}\right)_{freez\_rim} = -\frac{(1-RET)C_{liq}}{q_{liq}}\left(\frac{\partial q_{liq}}{\partial t}\right)_{freez\_rim} \tag{6}$$

which is a source for gas phase, while in the liquid and ice phase:

$$\left(\frac{\partial C_{liq}}{\partial t}\right)_{freez\_rim} = \frac{C_{liq}}{q_{liq}}\left(\frac{\partial q_{liq}}{\partial t}\right)_{freez\_rim} \tag{7}$$

$$\left(\frac{\partial C_{ice\_p}}{\partial t}\right)_{freez\_rim} = \frac{(RET)C_{liq}}{q_{liq}}\left(\frac{\partial q_{ice\_p}}{\partial t}\right)_{freez\_rim} \tag{8}$$

The tendency of liquid water (cloud or rain) by freezing and riming processes is negative and is a sink for liquid phase.

During the water vapor deposition on ice hydrometeors, the gaseous species can be partly buried into the growing crystal.

The burial coefficient β transfers material from gas to ice phase with the following rates:

$$\left(\frac{\partial C_g}{\partial t}\right)_{dep} = \frac{\beta C_g}{q_v}\left(\frac{\partial q_v}{\partial t}\right)_{dep\_vap\_ice} \tag{9}$$

$$\left(\frac{\partial C_g}{\partial t}\right)_{dep} = -\left(\frac{\partial C_{ice}}{\partial t}\right)_{dep} \tag{10}$$

*where in equations (6), (7), (8), (9), (10)* $C_{liq}$, $C_g$, $C_{ice\_p}$ *and* $C_{ice}$ *are the concentrations of chemical species respectively in liquid (rain or cloud water), gas and precipitating iced hydrometeors (snow or graupel) and all ice hydrometeors (molec.cm*$^{-3}$*).* $q_{liq}$, $q_v$, $q_{ice\_p}$ *are respectively the mixing ratio of water cloud or rain, vapor and graupel or snow (g/kg).*

# 3. Model set-up and results

## 3.1. Cloud features

In M2C2, the mixed-phase cloud is simulated using an entrainment rate of $4.7 \cdot 10^{-4}$ m$^{-1}$, which causes the air parcel to reach the altitude of 5 km in 10 minutes. This dynamical framework in favor of ice formation faithfully reproduces the one previously described by Audiffren et al. (1998) with temperature and dew point profiles from Reisin et al. (1996). The cloud event is characterized with specific CCN spectrum at 1% supersaturation which is representative of a moderate continental case, as described in Reisin et al. (1996) and furthermore will not precipitate very much. This case was selected to limit the wet scavenging of species by precipitation and emphasize the uptake of trace gases in mixed-phase cloud.

The 0°C isotherm is located around 2600 m. The convective air parcel starts at 600 m above ground level with temperature equal to 15°C. Cloud base and top are, respectively at the altitudes of 600 m and 5100 m where the temperature reaches -18°C. The main results for the moderate continental cloud are presented in Table 2. Compared to the model of Reisin et al. (1996), in our model, snow is considered and the hydrometeor number concentration is predicted. Despite these differences, general features are retrieved with a maximum updraft of 13 m/s, a maximum water content of 6 g/kg, 0.05 g/kg, and 4.3 g/kg respectively, for the maxima of cloud, ice pristine + snow and graupel. The run lasts approximately 20 min with the mature stage of the cloud between 5 min and 15 min followed by a decaying stage the last

five minutes where a net decrease in the cloud water content is observed, together with a slowing down of the riming process.

Figure 3a illustrates the relative water fractions for different phases as a function of time, normalized with respect to maximum liquid water content. The total liquid water content reached its maximum value five minutes from model initialization, at which time the graupel fraction was less than 0.1%. At the same time, the total water fraction (water + ice + snow + graupel) of the cloud reached its maximum.

Then, the graupel fraction rapidly increases as a result of graupel production by riming and drop freezing. Ten minutes later, most of the cloud fraction is in the form of graupel, while the drops fraction composed only 10% and the ice crystal a few percent. Snow fraction driven by ice growth, riming of raindrops on ice and of cloud droplets on snow steadily increases up to around 1% of the maximum liquid water content and decreases at the end of the simulation through precipitation and evaporation.

In Figure 3a, dotted curves represent the total liquid water content and the water fractions obtained for the same cloud than before but when neglecting ice phase processes. The total liquid water content is decreasing faster and the cloud is lasting longer than in the reference case when mixed-phase processes are activated.

In the same manner, the total water content and the water fractions are drawn in Figure 3b, for a case that will be studied in section 3.3 involving spherical crystals. Already, we can observe that the cloud duration is longer in the case of spherical crystals and this discrepancy will probably have some impact on gas scavenging (see section 4.2).

## 3.2. Chemical features

Initial data for the chemical species considered in the M2C2 model are given in Table 3. The gas phase chemical species are initialized using measurements from Voisin et al. (2000) who

characterized a winter continental cloud at mid-latitudes and performed experimental studies on retention coefficient for inorganic and organic chemical species during mixed-phase processes.

Figure 4a presents the time evolution of gas phase concentrations for specific chemical species, which have been selected to illustrate a representative range of chemical reactivities, retention efficiencies and solubility rates (Figure 2). $CH_2O$ is a stable terminal organic compound in gas phase, revealing the level of atmospheric oxidation capacity, $H_2O_2$ is one of the most reactive oxidant in aqueous phase (Daum et al., 1990) and HCOOH, $HNO_3$ are respectively weak and strong acids which influence pH of cloud water (Chameides and Davies, 1983; Schwartz, 2003). The species exhibit similar evolution with a strong decrease at the beginning of the run, when cloud appears and the various curves are organized with respect to solubility levels. $CH_2O$ is not scavenged as efficiently as $H_2O_2$, HCOOH and $HNO_3$. From 12:05 to 12:10, nitric acid concentration suddenly increases because at that time cloud droplets are converted into raindrops, leading to a less efficient mass transfer from gas phase to rain phase together with efficient gas phase production of nitric acid by the reaction with OH and $NO_2$. At those times, the cloud is supercooled with liquid phase still present. Later on, the temperature and the total condensed water decrease and ice forms and a global increase of gas concentrations is observed for all species. However, only $CH_2O$ and HCOOH almost retrieve their initial concentration levels due to their low retention in the ice phase.

Several factors are of importance in driving the final composition of cloud ice and include the partitioning of species between gaseous and supercooled liquid phases, the amount of rimed ice collected by snowflakes, and the retention of gas during shock freezing of supercooled droplets onto ice particles. Strong acids such as $HNO_3$, being sufficiently soluble in water, are mainly partitioned into supercooled water droplets. Furthermore, being subsaturated in liquid droplets, these species are well retained in rimed ice. For these species, riming is found to be

the main process driving the final composition of snowflakes, direct incorporation from the gas phase during growth of snowflakes remaining insignificant because of low concentrations in the gas phase (Voisin et al., 2000).

Figure 4b presents the evolution of gaseous $CH_2O$, $H_2O_2$, $HNO_3$ and HCOOH but this time as a function of temperature along the whole simulation. According to temperature, two regimes can be differentiated with liquid phase processes for temperatures greater than about -5°C and with ice phase processes otherwise. The evolution of concentration in Figure 4b reflects the temperature-dependent solubility of chemical species for temperatures comprised between -5°C and 15°C. For negative temperatures (below -5°C) the amount of gaseous chemical species is modified by the presence of ice phase: chemical species depending on retention and burial coefficients are partially retained in the ice (more particularly the acidic species in Figure 2). The warming of the descending parcel creates a kind of hysteresis, which occurs when temperature starts to increase (around -18°C) and is directly linked to the efficiency of chemical species retention by ice for temperatures ranging from -18°C to -5°C.

## 3.3. Sensitivity tests

To get insights in the relative effects of ice processes, retention, burial, crystal shapes on gas scavenging, it is interesting to proceed to sensitivity tests. Four simulations have been performed in addition to the reference case which considers complex crystal geometry, a burial efficiency of 1, a variable retention coefficient as defined in Figure 2 and Section 2.4, mixed-phase processes and is fully described in sections 3.1 and 3.2. Those sensitivity tests include the following departures from the reference case:

1) a warm simulation where ice processes are switched off;
2) a case where the burial efficiency is set to 0;
3) a case where the retention efficiency is set equal to 1 for all chemical species;

4) a case where ice crystals are considered as spheres.

Figure 5 shows the time evolution of gas concentrations for (a) $CH_2O$, (b) $H_2O_2$, (c) $HNO_3$ and (d) HCOOH as in Figure 4a, but zooming on the end of the simulation when ice processes can occur. One point that has to be raised is the abrupt changes in gas concentration that are observed at times denoted by the arrows on Figure 5, and that corresponds to cloud water decrease observed in every run (reference case, case without ice and case with spherical crystals). The first main result is that burial is ineffective to scavenge all gases considered in our study by comparing case 2 with the reference case. Considering a full retention in ice for all species, obviously does not affect nitric acid but leads to large discrepancies for HCHO, $H_2O_2$ and HCOOH compared to their original retention coefficients respectively equal to 0.02, 0.5 and to $0.012+0.0058(T-T_0)$, as drawn in Figure 2. Their evolution with time before the decrease of cloud water amount just reflects that, when graupels form, they are fully retained in ice phase. Then, the time evolution is different for these three species due to the competition between gas phase reactivity, exchanges between gas and liquid phases and aqueous phase reactivity.

Large deviations are observed between the run with and without ice for all compounds. For chemical species with a small retention coefficient (HCHO, $H_2O_2$ and HCOOH), their gaseous concentrations are smaller when no ice is considered because, in this case, soluble species are scavenged by cloud water whereas in the reference case, no more cloud water is available and species are released back to the gas phase when liquid water freezes. $H_2O_2$ has a contrasted behavior than the other compounds, at the end of the reference simulation. Its concentration increases as the total condensed water is depleted and then decreases when ice stabilizes in the form of graupels. The only possibility for $H_2O_2$ concentration to decrease is its reactivity with OH and its direct photolysis. In the meantime, nitric acid is produced from the gas phase reaction between $NO_2$ with OH radical. This continuous production explains the

difference between the runs with and without ice for nitric acid: neglecting ice, nitric acid produced in gas phase is scavenged at once by cloud droplets whereas when ice is considered, burial is inefficient to scavenge nitric acid from the ice phase.

The influence of crystal shape is similar for all gases with a shift in time for the gas content evolution, due to different riming intensity of the regular versus complex crystals, as will be discussed in Section 4.2.

# 4. Impacts of ice microphysics on chemistry

## 4.1. Retention and burial processes

As discussed previously (section 3), two processes have been highlighted in the treatment of gas uptake by ice hydrometeors: gas retention which occurs for retaining a fraction of gas during the freezing/riming processes and burial which depicts the entrapment of gas in ice crystals during their growth by vapor diffusion. For this reason, special attention is now given to these particular microphysical pathways.

Figure 6a presents the main microphysical processes involved in the evolution of ice hydrometeors, which influence burial and retention and determines gas partitioning among phases as a function of temperature. Freezing is negligible over the whole simulation because of small continental cloud droplets.

Water vapor deposition on graupel, which drives the burial process, initially dominates for temperatures below -10°C. Riming causes ice crystals to grow by accretion (collection growth) and is represented in Figure 6a. Collection growth by cloud water on ice hydrometeors is the most efficient process when temperature is below -8°C, around -14°C with a predominant importance of riming on graupel (COLLQCG). This will strongly influence retention of gases by ice crystals. These processes are effective when the mixing

ratio of graupel, snow and ice become important i.e. after 10 min of simulation time (Figure 3).

Figure 6b illustrates the influence of retention and burial on different chemical species with various solubilities and retention coefficients (see Figure 2), through the production or destruction rates in $s^{-1}$, which exchange chemical matter between liquid phase, ice phase and gas phase and expressed by $\frac{1}{C_g}(\frac{\partial}{\partial t}C_g)_{RET\_BUR}$

*where $C_g$ is the gas concentration (molec.cm$^{-3}$) ; $(\frac{\partial}{\partial t}C_g)_{RET\_BUR}$ is the temporal variation of gas concentration related to burial and retention effects (molec.cm$^{-3}$.s$^{-1}$).*

Since nitric acid has retention coefficient equal to one, it is totally transferred from liquid water to ice when riming occurs, and the only effect that could be seen on Figure 6a is the effect of burial. This effect of burial on nitric acid is insignificant as seen in Figure 6a, on the right hand scale: this confirms that burial effect is negligible. For others species, significant contribution can only come from the retention effect, which occurs for temperatures less than -10°C and leads to a maximum value for temperatures between -15°C and -13°C. Degassing is larger for $H_2O_2$ and HCOOH than for $CH_2O$. The shift and the intensity for each chemical species peaks depend on solubility and retention coefficient.

## 4.2. Influence of crystal shape on gas scavenging

In the previous section, retention has been identified as the main process that drives the partitioning of gases between gas, liquid and ice phases. By definition, retention is strongly linked to riming and freezing processes.

So it is important to consider the complex structures of ice crystals since they have in reality a variety of habits, while riming changes and modifies the properties of ice particles. This has been shown by Heymsfield et al. (2007) who collected observations sampled for a wide range

of temperatures and by Barthazy and Schefold (2006) who measured fall velocities of graupel and of snowflakes of different riming degree and consisting of different crystal types.

Also, various habits for ice particles lead to fall velocity differences that directly impact on the residence time and fallout precipitation which both regulate the gas scavenging efficiency. One recent study from Michael and Stuart (2009) concludes that no clear effect was observed on retention in case of hail probably due to very efficient ice-liquid interface supercooling.

The uptake of inorganic compounds like HCl, $HNO_3$, and $SO_2$ by planar ice surfaces, ice spheres, and dendritic ice crystals during crystal growth have been already reported (Mitra et al., 1990; Diehl et al., 1995; Conklin et al., 1993; Domine and Thibert, 1996; Santachiara et al., 1998). However, data on the uptake of organic compounds during crystal growth are rather limited (Fries et al., 2007) and all these experimental studies do not allow for quantifying the effect of crystal shape on the efficiency of gas uptake.

This section is devoted to sensitivity tests that highlight the importance of riming and consequently of gas retention as a function of crystal shape.

For this, we compared the reference case described in the previous section and assuming non-spherical particles (Table 1) with a new simulation performed with hypothesis of spherical snow and graupel particles. Time evolution of the various hydrometeors contents is presented in Figure 3b, for an easier comparison with the reference case.

As seen before in Figure 6a, retention is driven by the growth of graupel by cloud water collection on graupel (COLLQCG) and this is still true for ice crystals with spherical geometry. To evaluate the influence of crystal shape on riming and thereby retention processes, evolution of graupel mixing ratio is followed by looking at the rimed mass fraction of all particles defined as:

$$RI = \frac{q_{graup}}{q_{snow} + q_{graup} + q_{ice} + q_{cw}} \qquad (12)$$

*where $q_{graup}$, $q_{snow}$, $q_{ice}$ and $q_{cw}$ are the mixing ratios for graupel, snow, ice and cloud water respectively ($g.kg^{-1}$).*

This ratio defines the riming intensity as described in Lin and Colle (2008) and ranges from 0 (pristine ice particles) to 1 (graupel). Figure 7 displays the evolution of this ratio as a function of the temperature for the two simulations with non-spherical and spherical hypothesis for the crystal shapes. The growth of graupel by cloud water collection on graupel (COLLQCG) is also shown in both cases. In the non-spherical case, riming is much more important when the temperature gets colder (-17°C à -12°C) while in the spherical case COLLQCG is smaller but is spread over a larger range of temperatures (from -17°C to -9°C).

The riming intensity is larger in the non-spherical case vs. the spherical one because it is directly determined by the mean size and the terminal velocity of graupels. Figure 8 presents the evolution of graupel mean sizes and terminal velocities in the two simulations with spherical and non-spherical assumptions for graupels. The double prediction of mixing ratios and number concentrations of ice particles, allows for the knowledge of the crystal mean diameter at every time step in the simulation. This mean diameter is used to calculate the terminal fall velocities for the various ice particles as defined in Table 1. Graupels with complex shape are larger for temperatures above -16°C, they become heavier and have larger terminal velocities since their mass and velocity are directly related to the size. Due to these properties, the collection growth of non-spherical graupel by cloud water on graupel is more efficient and quicker over that range of temperatures than in the case with spherical particles.

The strong dependency of the retention on the collection growth of graupel by cloud water on graupel (COLLQCG) is now illustrated. Figure 6b shows the evolution of the retention and burial rates for different chemical species with various solubilities, for spherical ice particles with dotted lines and can be compared with solid lines showing the equivalent rates for non-spherical ice particles. The production rates in $s^{-1}$ describing the exchanges of chemical

species between ice phase and gas phase are larger and spread over a smaller range of temperatures in the non-spherical reference case (Figure 6b, solid lines) than in the spherical case (Figure 6b dotted lines). They reflect the behavior of the collection growth of graupel by cloud water on graupel (COLLQCG) previously discussed. Comparing the two figures, for all species considered, degassing is larger for non-spherical crystals than for spherical ones. For temperatures ranging from -18°C to -11°C, non-spherical graupels are growing faster than spherical ones as seen in Figure 6b. Also, the riming intensity in Figure 7 peaks at colder temperatures for non-spherical crystals than spherical ones. This results in a more efficient degassing for non-spherical graupels.

The uptake of nitric acid in ice is more efficient when the riming intensity reaches its maximum (Figure 6) and when the graupel diameter does not increase anymore (Figure 7). It is also greater for non-spherical crystals that are much larger in size than spherical ones. These findings are in agreement with experimental observations done by Hoog et al. (2007) who concluded that uptake of gases by ice is the most efficient for nitric acid for non-growing crystals, even if it is rather small compared to uptake by water droplets.

## 5. Conclusion and discussion

In this paper, a multiphase cloud chemistry model M2C2 is presented with new developments including two-moment mixed-phase microphysics coupled with explicit chemistry. Partitioning of chemical species among gas, cloud, rain, and ice, snow and graupel is investigated to document gas-ice transfer, redistribution of chemical species by microphysical processes.

First, the importance of ice phase processes against liquid only processes leads to a very different gas budget for all species considered (HCOOH, $HNO_3$, $H_2O_2$, $CH_2O$). Several factors have been studied as possible contribution of the final composition of mixed-phase

clouds: temperature dependency of the chemical rates (reactivity and solubility), entrapment (retention and burial) of gases in ice particles, retention coefficient and solubilities of gases,

The main conclusions of the paper are: retention is the important process for all species, retention depends on the riming intensity which is determined by the collection growth of graupel by cloud droplets on rimed ice particles. Additionally, it is found that burial is negligible. Collection growth is found to be very sensitive to crystal shape, because varying mass-diameter relationships and terminal velocity dependencies on diameter is allowed with a two-moment microphysical parameterization. From our study which considers a mixed-phase cloud, it can be concluded that not the direct uptake by ice crystals but rather riming seems to be the major process for the scavenging of gases from the atmosphere via the ice phase. This work confirms the primordial role of retention in the chemical budget of soluble chemical species in the mixed-phase clouds. Further experimental efforts are needed to document the retention coefficients of other compounds apart from acids.

Even if our study shows a negligible effect of direct uptake of gas by crystals, these conclusions are not valid for the only glaciated part of mixed-phase clouds (anvil of convective clouds for instance) and for cirrus. Processes of gas-ice mass transfer include adsorption on non-growing ice hydrometeors surfaces (Tabazadeh et al., 1999), co-deposition with water vapor on growing ice (Fries et al., 2007), dissolution in a quasi-liquid layer on ice surface (Michael and Stuart, 2009; Abbatt, 2003), diffusion in the bulk ice and incorporation into the crystal structure (Kärcher and Basko, 2004). These processes are poorly understood or have been studied in laboratories with artificial ice and for temperatures that are far from real tropospheric conditions. A quantitative physical understanding of the interactions of snow and ice with trace gases is critical for predicting the effects of climate change on atmospheric composition, and for modeling atmospheric chemistry (McNeill and Hastings, 2008). Additional laboratory investigations are urgently needed to provide elements for

validating parameterizations of gas scavenging by growing ice particles (Kärcher et al., 2009; Marécal et al., 2010). They could include experiments with different temperatures in the range of tropospheric conditions to reproduce different conditions of crystal growth and could concern a wider range of species, possibly being able to react between them.

## 6. Acknowledgments

Computer resources were provided by IDRIS (Institut du Développement et des Ressources en Informatique Scientifique) and by CINES (Centre Informatique de l'Enseignement Supérieur), project n°15090.

# LIST OF SYMBOLS

| Notation | Description | Unit |
|---|---|---|
| D1 | Distribution factor between graupel and snow | |
| CONDQCW | Growth of water vapor by evaporation of cloud water | $g.kg^{-1}.s^{-1}$ |
| | Growth of cloud water by condensation of water vapor | |
| EVAPMQS | Growth of water vapor by snow evaporation | $g.kg^{-1}.s^{-1}$ |
| EVAPMQG | Growth of water vapor by graupel evaporation | $g.kg^{-1}.s^{-1}$ |
| CONDQRW | Growth of water vapor by evaporation of rain | $g.kg^{-1}.s^{-1}$ |
| | Growth of rain by condensation of water vapor | |
| QCWNUC | Growth of water cloud by nucleation of cloud water | $g.kg^{-1}.s^{-1}$ |
| MELTQI | Growth of cloud water by melting of ice | $g.kg^{-1}.s^{-1}$ |
| AUTOCQRW | Growth of rain by autoconversion of cloud water | $g.kg^{-1}.s^{-1}$ |
| ACCREQRW | Growth of rain by accretion of cloud water on rain | $g.kg^{-1}.s^{-1}$ |
| XMELTQS | Growth of rain water by melting of snow | $g.kg^{-1}.s^{-1}$ |
| XMELTQG | Growth of rain water by melting of graupel | $g.kg^{-1}.s^{-1}$ |
| XMELTRG | Growth of rain water by graupel collection on rain water | $g.kg^{-1}.s^{-1}$ |
| XMELTCG | Growth of rain water by snow collection on cloud water | $g.kg^{-1}.s^{-1}$ |
| SEDQRW | Sedimentation of rain water | $g.kg^{-1}.s^{-1}$ |
| XNUCQI | Growth of ice by heterogeneous nucleation of water vapor | $g.kg^{-1}.s^{-1}$ |
| FREZQI | Growth of ice by heterogeneous freezing of cloud water | $g.kg^{-1}.s^{-1}$ |
| DEPVQI | Growth of ice by water vapor deposition on ice | $g.kg^{-1}.s^{-1}$ |
| RIMQI | Growth of ice by water cloud collection on ice | $g.kg^{-1}.s^{-1}$ |
| XICEMQS | Growth of ice by the ice splinter multiplication process with snow | $g.kg^{-1}.s^{-1}$ |
| XICEMQG | Growth of ice by the ice splinter multiplication process with | $g.kg^{-1}.s^{-1}$ |

| | | |
|---|---|---|
| | graupel | |
| COLLQIRG*D1 | Growth of snow by ice collection on rain water | $g.kg^{-1}.s^{-1}$ |
| COLLQRIG*D1 | Growth of snow by rain water collection on ice | $g.kg^{-1}.s^{-1}$ |
| COLLQRSS | Growth of snow by ice collection on rain water | $g.kg^{-1}.s^{-1}$ |
| COLLQIS | Growth of snow by ice collection on snow | $g.kg^{-1}.s^{-1}$ |
| COLLQCSS | Growth of snow by cloud water collection on snow | $g.kg^{-1}.s^{-1}$ |
| DEPQSNOW | Growth of snow by water vapor deposition on snow | $g.kg^{-1}.s^{-1}$ |
| FORMQS | Growth of snow by conversion of ice into snow | $g.kg^{-1}.s^{-1}$ |
| SEDQS | Sedimentation of snow | $g.kg^{-1}.s^{-1}$ |
| FREZQR | Growth of graupel by heterogeneous freezing of rain water | $g.kg^{-1}.s^{-1}$ |
| COLLQIRG*(1-D1) | Growth of graupel by ice collection on rain water | $g.kg^{-1}.s^{-1}$ |
| COLLQRIG*(1-D1) | Growth of graupel by rain water collection on ice | $g.kg^{-1}.s^{-1}$ |
| COLLQSRG | Growth of graupel by snow collection on rain water | $g.kg^{-1}.s^{-1}$ |
| COLLQRSG | Growth of graupel by rain water collection on snow | $g.kg^{-1}.s^{-1}$ |
| COLLQCSG | Growth of graupel by cloud water collection on snow | $g.kg^{-1}.s^{-1}$ |
| COLLQCG | Growth of graupel by cloud water collection on graupel | $g.kg^{-1}.s^{-1}$ |
| COLLQRG | Growth of graupel by rain water collection on graupel | $g.kg^{-1}.s^{-1}$ |
| DEPQGRAUP | Growth of graupel by water vapor deposition on graupel | $g.kg^{-1}.s^{-1}$ |
| RIMQG | Growth of graupel by water cloud collection on ice | $g.kg^{-1}.s^{-1}$ |
| RIMQIG | Growth of graupel by ice collection on water cloud | $g.kg^{-1}.s^{-1}$ |
| SEDQG | Sedimentation of graupel | $g.kg^{-1}.s^{-1}$ |

# REFERENCES


Abbatt, J.P.D., 2003. Interactions of atmospheric trace gases with ice surfaces: Adsorption and reaction. Chem. Rev., 103, 4783-4800.

Abdul-Razzak, H., Ghan, S.J., 2000. A parameterization of aerosol activation. II. Multiple aerosol types. J. Geophys. Res., 105, 6837-6844.

Ackerman, T.P., Liou, K.P.F.P, Valero J., Pfister L., 1998. Heating rates in tropical anvils. J. Atmos. Sci., 45, 1606-1628.

Audiffren, N., Renard, M., Buisson, E., Chaumerliac, N., 1998. Deviations from the Henry's law equilibrium during cloud events: a numerical approach of the mass transfer between phases and its specific numerical effects. Atmos. Res., 49, 139-161.

Audiffren, N., Cautenet, S., Chaumerliac, N., 1999. A Modeling Study of the Influence of Ice Scavenging on the Chemical Composition of Liquid-Phase Precipitation of a Cumulonimbus Cloud. J. Appl. Meteor., 38, 1148-1160.

Barth, M.C., Stuart, A.L., Skamarock, W.C., 2001. Numerical simulations of the July 10, 1996, Stratospheric-Tropospheric Experiment: Radiations, Aerosols, and Ozone (STERAO)-Deep Convection experiment storm: Redistribution of soluble tracers. J. Geophys. Res., 106(D12), 12381-12400.

Barth, M.C., Hess, P.G., Madronich, S., 2002. Effect of marine boundary layer clouds on tropospheric chemistry as analyzed in a regional chemistry transport model. J. Geophys. Res., 107(D11), 4126.

Barthazy, E., Schefold, R., 2006. Fall velocity of snowflakes of different riming degree and crystal types. Atmos. Res., 82, 391-398.

Barthe, C., Molinié, G., Pinty, J.P., 2005. Description and first results of an explicit electrical scheme in a 3D cloud resolving model. Atmos. Res., 76, 95-113.

Berry, E.X., Reinhardt, R.L., 1974a. An analysis of cloud drops growth by collection: Part I. Double distributions. J. Atmos. Sci., 31, 1814-1824.

Berry, E.X., Reinhardt, R.L., 1974b. An analysis of cloud drops growth by collection: Part II. Single initial distributions. J. Atmos. Sci., 31, 1825-1831.

Berry, E.X., Reinhardt, R.L., 1974c. An analysis of cloud drops growth by collection: Part III. Accretion and self collection. J. Atmos. Sci., 31, 2118-2126.

Berry, E.X., Reinhardt, R.L., 1974d. An analysis of cloud drops growth by collection: Part IV. A new parametrization. J. Atmos. Sci., 31, 2127-2135.

Caro, D., Wobrock, W., Flossmann, A.I., Chaumerliac, N., 2004. A two-moment parameterization of aerosol nucleation and impaction scavenging for a warm cloud microphysics: description and results from a two-dimensional simulation. Atmos. Res., 70, 171-208.

Chameides, W.L., Davies, D.D., 1983. The coupled gas phase/aqueous phase free radical chemistry of a cloud. In Precipitation Scavenging , Dry Deposition and Resuspension (edited by Pruppacher H.R., Semonin R.G., Slinn W.G.N.), Elsevier, New York, 431-443.

Chaumerliac, N., Richard, E., Pinty, J.P., Nickerson, E.C., 1987. Sulfur scavenging in a mesoscale model with quasi-spectral microphysics: Two dimensional results for continental and maritime clouds. J. Geophys. Res., 92, 3114-3126.

Chen, J.P., Lamb, D., 1990. The role of precipitation microphysics in the selective filtration of air entering the upper troposphere, 1990 Conference on Cloud Physics. Am. Meteorol. Soc., 479-484.

Conklin, M.H., Sommerfeld, R., Laird, S.K., Villinski, J.E., 1993. Sulphur dioxide reactions on ice surface: implications for dry deposition to snow. Atmos. Envir., 27A, 1159-1166.

Cooper, W.A., 1986. Ice initiation in natural clouds. Precipitation Enhancement-A Scientific Challenge. Am. Meteorol. Soc., 29-32.

Cotton, W.R., Alexander, G.D., Hertenstein, R., Walko, R.L., McAnelly, R.L., Nicholls, M., 1995. Cloud venting — A review and some new global annual estimates. Earth-Science Reviews, 39, 169-206.

Daum, P.H., Kleinman, L.I., Hills, A.J., Lazrus, A.L., Leslie, A.C.D., Busness, K., Boatman, K., 1990. Measurement and interpretation of concentrations of $H_20_2$ and related species in the upper Midwest during summer. J. Geophys. Res., 95(D7), 9857-9871.

Deguillaume, L., Leriche, M., Monod, A., Chaumerliac, N., 2004. The role of transition metal ions on $HO_x$ radicals in clouds: a numerical evaluation of its impact on multiphase chemistry. Atmos. Chem. Phys., 4, 95-110.

Deguillaume, L., Leriche, M., Chaumerliac, N., 2005. Impact of radical versus non-radical pathway in the Fenton chemistry on the iron redox cycle in clouds. Chemosphere, 60, 718-724.

Diehl, K., Mitra, S.K., Pruppacher, H.R., 1995. A laboratory study of the uptake of $HNO_3$ and HCl vapor by snow crystals and ice spheres at temperatures between 0 and -40°C. Atmos. Envir., 29, 975-981.

Dominé, F., Thibert, E., 1996. Mechanism of incorporation of trace gases in ice grown from the gas phase. Geophys. Res. Let., 23, 3627-3630.

Ferrier, B.S., 1994. A double-moment multiple-phase four-class bulk ice scheme. Part I: Description. J. Atmos. Sci., 51, 249-280.

Flossmann, A.I., Wobrock, W., 1996. Venting of gases by convective clouds. J. Geophys. Res., 101(D13), 639-649.

Fries, E., Starokozhev, E., Haunold, W., Jaeschke, W., Mitra, S.K., Borrmann, S., Schmidt, M.U., 2007. Laboratory studies on the uptake of aromatic hydrocarbons by ice crystals during vapor depositional crystal growth. Atmos. Envir., 41, 6156-6166.

Gérémy, G., Wobrock, W., Flossmann, A.I., Scharzenböck, A., Mertes, S., 2000. A modelling study on the activation of small Aitken-mode aerosol particles during CIME 97. Tellus B, 52, 959-979.

Hallet, J., Mossop, S.C., 1974. Production of secondary ice particles during the riming process. Nature, 249, 26-28.

Hegg, D.A., 2001. The impact of clouds on aerosols population. IGAC activities newsletter n°23, Avril 2001.

Heymsfield, A.J., Miloshevich, L.M., Twohy, C., Sachse, G., Oltmans., S., 1998. Upper tropospheric relative humidity observations and implications for cirrus ice nucleation. Geophys. Res. Let., 25, 1343-1346.

Heymsfield, A.J., Bansemer, A., Twohy, C., 2007. Refinements to ice particle mass dimensional and terminal velocity relationships for ice clouds: Part I: Temperature dependence. J. Atmos. Sci., 64, 1047-1067.

Hoog, I., Mitra, S.K., Diehl, K., Borrmann, S., 2007. Laboratory studies about the interaction of ammonia with ice crystals at temperatures between 0 and –20°C. J. Atmos. Chem., 57, 73-84.

Huthwelker, T., Ammann, M., Peter, T., 2006. The uptake of acidic gases on ice. Chem. Rev., 106, 1375-1444.

Iribarne, J.V., Pyshnov, T., 1990a. The effect of freezing on the composition of the supercooled droplets, I: Retention of HCl, $HNO_3$, $NH_3$, and $H_2O_2$. Atmos. Envir., 24A, 383-387.

Iribarne, J.V., Pyshnov, T., 1990b. The effect of freezing on the composition of the supercooled droplets, II: Retention of S(IV). Atmos. Envir., 24A, 389-398.

Kärcher, B., Basko, M.M., 2004. Trapping of trace gases in growing ice crystals. J. Geophys. Res.,,109, D22204.

Kärcher, B., Abbatt, J.P.D., Cox, R.A., Popp, P.J., Voigt, C., 2009. Trapping of trace gases by growing ice surfaces including surface-saturated adsorption, J. Geophys. Res. 114, D13306.

Lafore, J.P., Stein, J., Asencio, N., Bougeault, P., Ducrocq, V., Duron, J., Fischer, C., Hereil, P., Mascart, P., Pinty, J.P., Redelsperger, J.L., Richard, E., Vila-Guerau de Arellano, J., 1998. The Meso-NH Atmospheric Simulation System. Part I: Adiabatic formulation and control simulations. Annales Geophysicae, 16, 90-109.

Lamb, D., Blumenstein, R., 1987. Measurements of the entrapment of sulphur dioxide by rime ice. Atmos. Envir., 21, 1765-1772.

Lawrence, M.G., Crutzen, P.J., 1998. The impact of cloud particle gravitational settling on soluble trace gas distributions. Tellus B, 50, 263–289.

Leriche, M., Voisin, D., Chaumerliac, N., Monod, A., Aumont, B., 2000. A model for tropospheric multiphase chemistry: application to one cloudy event during the CIME experiment. Atmos. Envir., 35, 5015-5036.

Leriche, M., Chaumerliac, N., Monod, A., 2001. Coupling quasi-spectral microphysics with multiphase chemistry : case study of a polluted air mass at the top of the Puy de Dôme mountain (France). Atmos. Envir., 35, 5411-5423.

Leriche, M., Deguillaume, L., Chaumerliac, N., 2003. Modeling study of strong acids formation and partitioning in a polluted cloud during wintertime. J. Geophys. Res., 108(D14), 4433-4444.

Leriche, M., Curier, L.,R., Deguillaume, L., Caro, D., Sellegri, K., Chaumerliac, N., 2007. Numerical quantification of sources and phase partitioning of chemical species in cloud: application to

wintertime anthropogenic air masses at the Puy de Dôme station. J. Atmos. Chem., 57, 281-297.

Lin, Y., Colle, B.A., 2008. Development of a new bulk microphysical parameterization with varying riming intensity and its evaluation within WRF. 9th WRF Users' Workshop, June 23 – 27, Boulder.

Liu, H., Wang, P.K., Schlesinger, R.E., 2003. A numerical study of cirrus clouds. Part II: Effects of ambient temperature, stability, radiation, ice microphysics, and microdynamics on cirrus evolution. J. Atmos. Sci., 60, 1097-1119.

Marécal V., Pirre, M., Rivière, E.D., Pouvesle, N., Crowley, J. N., Freitas, S. R., Longo, K. M., 2010. Modelling the reversible uptake of chemical species in the gas phase by ice particles formed in a convective cloud. ACPD, 9, 24361–24410.

Mari, C., Jacob, D. J., and Bechtold, P., 2000. Transport and scavenging of soluble gases in a deep convective cloud. J. Geophys. Res., 105, 22 255–22 267.

McCumber, M., Tao, M.K., Simpson, R., Soong, S.T., 1991. Comparison of ice-phase microphysical parametrization schemes using numerical simulations of tropical convection. J. Appl. Meteorol., 30, 985-1004.

McNeill, V.F., Hastings, M.G., 2008. Ice in the environment: connections to atmospheric chemistry. Environ. Res. Lett., 4, 045004.

Meyers, M.P., Walko, R.L., Harrington, J.Y., Cotton, W.R., 1997. New RAMS cloud microphysics parametrization Part II: the two-moment scheme. Atmos. Res., 31, 29-62.

Michael, R., Stuart, A.L., 2009. The fate of volatile chemicals during wet growth of a hailstone. Environ. Res. Lett., 4, 1748-9326.

Mitra, S.K., Barth, S., Pruppacher, H.R., 1990. A laboratory study on the scavenging of $SO_2$ by snow crystals. Atmos. Envir., 9, 2307-2312.

Morrison, H., Grabowski, W., 2008. Modeling Supersaturation and Subgrid-Scale Mixing with Two-Moment Bulk Warm Microphysics. J. Atmos. Sci., 65, 792–812.

Pruppacher, H.R., Klett J.D., 1997. Microphysics of clouds and precipitation, Kluwer Academic Publishers.

Reisin, T., Levin, Z., Tzivion, S., 1996. Rain production in convective clouds as simulated in an

axisymmetric model with detailed microphysics. Part II: effect of varying drops and ice initiation. J. Atmos. Sci., 53, 1815-1837.

Reisner, J., Rasmussen, R.M., Bruintjes, R.T., 1998. Explicit forecasting of supercooled liquid water in winter storms using the MM5 mesoscale model. Q. J. R. Meteorol. Soc., 124, 1071-1107.

Rutledge, S.A., Hobbs, P.V., 1984. The Mesoscale and Microscale Structure and Organization of Clouds and Precipitation in Midlatitude Cyclones. XII: A Diagnostic Modeling Study of Precipitation Development in Narrow Cold-Frontal Rainbands. J. Atmos. Sci., 41, 2949-2972.

Rutlegde, S.A., Hegg, D.A., Hobbs, P.V., 1986. A numerical model for sulfur and nitrogen scavenging in narrow cold-frontal rainbands 1. Model description and discussion of microphysical fields. J. Geophys. Res., 91(D13), 14385-14402.

Salzmann, M., Lawrence, M.G., Phillips, V.T.J., Donner, L.J., 2007. Model sensitivity studies regarding the role of the retention coefficient for the scavenging and redistribution of highly soluble trace gases by deep convective cloud systems. Atmos. Chem. Phys., 7, 2027-2045.

Sander, R., 1999. Compilation of Henry's Law Constants for Inorganic and Organic Species of Potential Importance in Environmental Chemistry (Version 3) http://www.henrys-law.org.

Santachiara, G., Prodi, F., Udisti, R., Prodi, A., 1998. Scavenging of $SO_2$ and $NH_3$ during growth of ice. Atmos. Res., 47-48, 209-217.

Sander, S.P., Finlayson-Pitts, B.J., Friedl, R.R., Golden, D.M., Huie, R.E., Keller-Rudek, H., Kolb, C.E., Kurylo, M.J., Molina, M.J., Moortgat, G.K., Orkin, V.L., Ravishankara, A.R., Wine, P.H., 2006. Chemical Kinetics and Photochemical Data for Use in Atmospheric Studies, Evaluation Number 15, JPL Publication 06-2, Jet Propulsion Laboratory, Pasadena.

Schwartz, S.E., 1986. Mass-Transport considerations pertinent to aqueous phase reactions of gases in liquid water cloud. Jaeschke, W., (Ed.), Chemistry of Multiphase Atmospheric Systems, NATO ASI Series, G6, Springer, Berlin.415-472.

Schwartz, S.E., 2003. Cloud Chemistry. In Handbook of Weather, Climate, and Water, Potter T. D. and Colman B. R., Eds., Wiley, 355.

Snider, J.R., Montague, D.C., Vali, G., 1992. Hydrogen peroxide retention in rime ice. J. Geophys. Res., 97(D7), 7569-7578.

Tabazadeh, A., Jensen, E.J., Toon, O.B., 1999. A surface chemistry model for nonreactive trace gas adsorption on ice: Implications for nitric acid scavenging by cirrus. Geophys. Res. Let., 26, 2211-2214.

Tao, W.K., 2003. Goddard cumulus ensemble (GCE) model: Application for understanding precipitation processes. Meteorol. Mono., 29, 107.

Thompson, G., Rasmussen, R.M., Manning, K., 2004. Explicit Forecasts of Winter Precipitation Using an Improved Bulk Microphysics Scheme. Part I: Description and Sensitivity Analysis. Mon. Wea. Rev., 132, 519-542.

Thompson, G., Field, P., Hall B., Rasmussen, R.M, 2006. A New Bulk Microphysical Parameterization in WRF. 7th WRF Users' Workshop, Boulder CO, June 2006.

Voisin, D., Legrand, M., Chaumerliac, N., 2000. Scavenging of acidic gases (HCOOH, $CH_3COOH$, $HNO_3$, HCl, and $SO_2$) and ammonia in mixed liquid-solid water clouds at the Puy de Dôme mountain (France). J. Geophys. Res., 105(D5), 6817-6835.

Wang, C., Chang, J.S., 1993. A Three-Dimensional Numerical Model of Cloud Dynamics, Microphysics, and Chemistry 4. Cloud Chemistry and Precipitation Chemistry. J. Geophys. Res., 98(D9), 16799-16808.

Willoughby, H.E., Jorgensen, D.P., Black, R.A, Rosenthal, S.L., 1985. Project STORMFURY: a scientific chronicle 1962–1983. Bull. Am. Meteorol. Soc., 66, 505-514.

Woods, C.P., Stoelinga, M.T., Locatelli, J.D., Hobbs, P.V., 2007. The IMPROVE-1 storm of 1–2 February 2001. Part III: Sensitivity of a mesoscale model simulation to the representation of snow particle types and testing of a bulk microphysical scheme with snow habit prediction. J. Atmos. Sci., 64, 3927-3948.

Yin, Y., Carslaw, K.S, Parker, D.J., 2002. Redistribution of trace gases by convective clouds mixed-phase processes. Atmos. Chem. Phys., 2, 293-306.

# LIST OF TABLES



# LIST OF FIGURES

- Figure 5: Time evolution of gas concentrations for $CH_2O$, HCOOH, $H_2O_2$, $HNO_3$ for several simulations: the reference case (solid line), a case without ice, a case considering spherical crystals, a case neglecting burial, a case assuming full retention.
- Figure 6: a) Microphysical rates related to the riming, freezing and deposition processes versus temperature (note that collection growth of graupels by cloud droplets on graupel is one order of magnitude larger than the other rates on the right-hand side scale).

  b) Evolution of gas species destruction or production rates $\frac{1}{C_g}(\frac{\partial}{\partial t}C_g)_{RET\_BUR}$ due to retention and burial effects as a function of temperature. Those rates correspond to the microphysical conversion rates shown in Figure 6a. Also, they are superimposed with the rates obtained for the simulation with spherical crystals (dashed lines).
- Figure 7: Riming intensity for non-spherical (in black) and spherical (in red) cases versus temperature. The collection growth rate of graupel by cloud water on graupel COLLQCG is also drawn versus temperature (right-hand side scale).
- Figure 8: Graupel diameter and terminal velocity for non-spherical (in black) and spherical (in red) cases versus temperature.

| | Non-spherical | | | Spherical | | |
|---|---|---|---|---|---|---|
| | Pristine | Snow | Graupel | Pristine | Snow | Graupel |
| a | 262 | 0.02 | 19.6 | 262 | 52.40 | 209.6 |
| b | 3 | 1.9 | 2.8 | 3 | 3 | 3 |
| c | 700 | 5.1 | 124 | 700 | 11.72 | 19.30 |
| d | 1 | 0.27 | 0.66 | 1 | 0.41 | 0.37 |

*Table 1 : Values of the a,b,c,d coefficients used in the formula of the crystal mass, given by $aD^b$ (kg) and of the fall velocity given by $cD^d(\rho_0/\rho_a)^{0,4}$ (m/s), as a function of crystal diameter. These data are provided by Lafore et al. (1998) and Barthe et al. (2005).*

| Parameters | | Values |
|---|---|---|
| CCN spectrum : $N = C.S^k$ | C ($cm^{-3}$) | 600 |
| | k | 0.7 |
| Maximum updraft (m/s) | | 13 |
| Location (m) | | 2500 |
| Cloud duration (min) | | 14 |
| Maximum mixing ratio (g/kg) | Cloud | 5.6 |
| | Ice | $7.4.10^{-3}$ |
| | Snow | $4.2.10^{-2}$ |
| | Graupel | 4.3 |
| Maximum number concentration ($cm^{-3}$) | Cloud | $6.00.10^9$ |
| | Ice | $7.77.10^4$ |
| | Snow | $4.05.10^4$ |
| | Graupel | $4.12.10^4$ |
| Mean diameter (m) | Cloud | $2.28.10^{-5}$ |
| | Ice | $4.10.10^{-5}$ |
| | Snow | $5.7.10^{-5}$ |
| | Graupel | $3.77.10^{-4}$ |

*Table 2: Main results for the moderate continental case simulation.*

| Chemical species in gaseous phase | Concentration ppbv |
|---|---|
| $N_2$ | $7.9 \cdot 10^8$ |
| $O_2$ | $2.13 \cdot 10^8$ |
| $H_2O$ | $1.79 \cdot 10^7$ |
| $O_3$ | 37.5 |
| NO | 0.95 |
| $NO_2$ | 6.28 |
| $CH_4$ | $1.72 \cdot 10^3$ |
| CO | 142 |
| $CO_2$ | $3.34 \cdot 10^5$ |
| $HNO_3$ | 0.15 |
| $H_2O_2$ | 0.07 |
| $CH_2O$ | 1.01 |
| $SO_2$ | 0.46 |
| CHO(OH) | 0.28 |
| $CH_3(OOH)$ | 1.01 |
| $CH_3OH$ | 2.28 |
| $NH_3$ | 0.13 |
| HCl | 0.07 |

*Table 3: Chemical initial concentrations for gas phase compounds in the M2C2 model.*

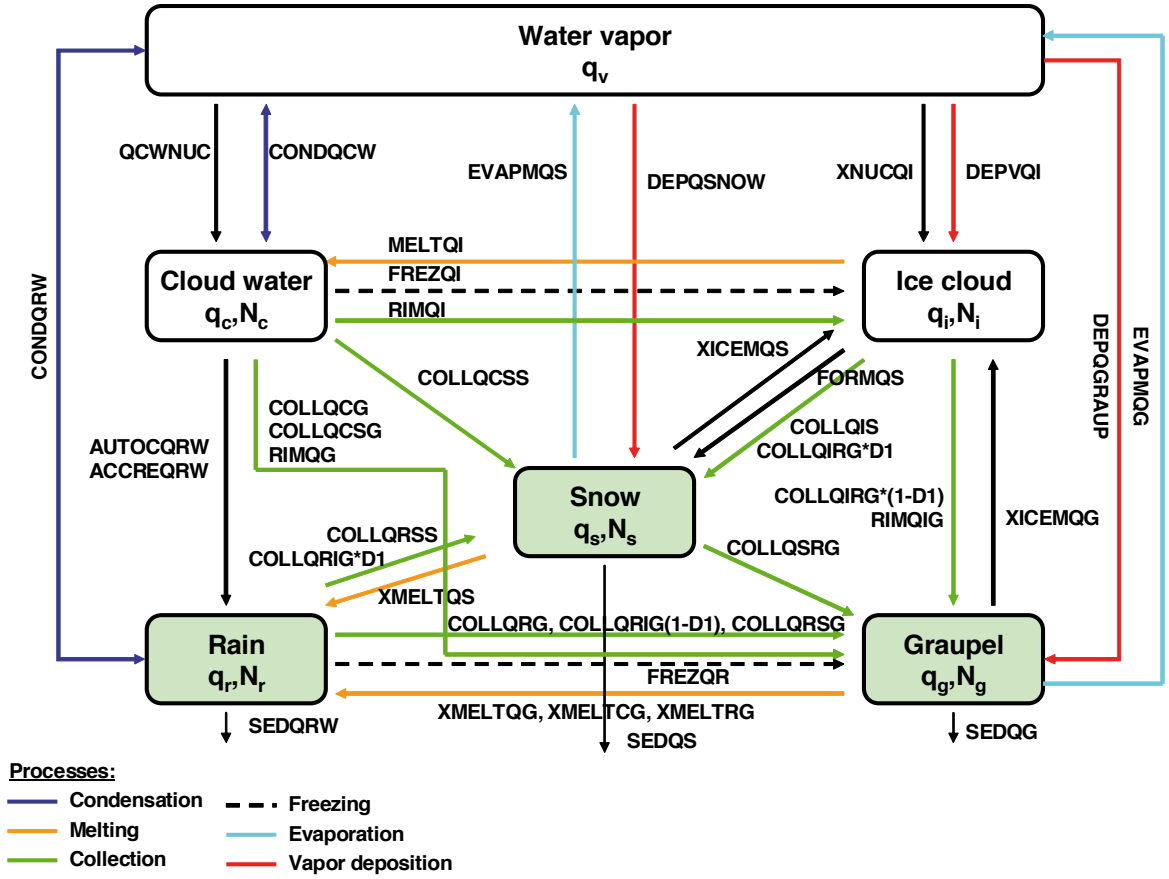


*Figure 1: Microphysical exchanges between various phases considered in the model.*

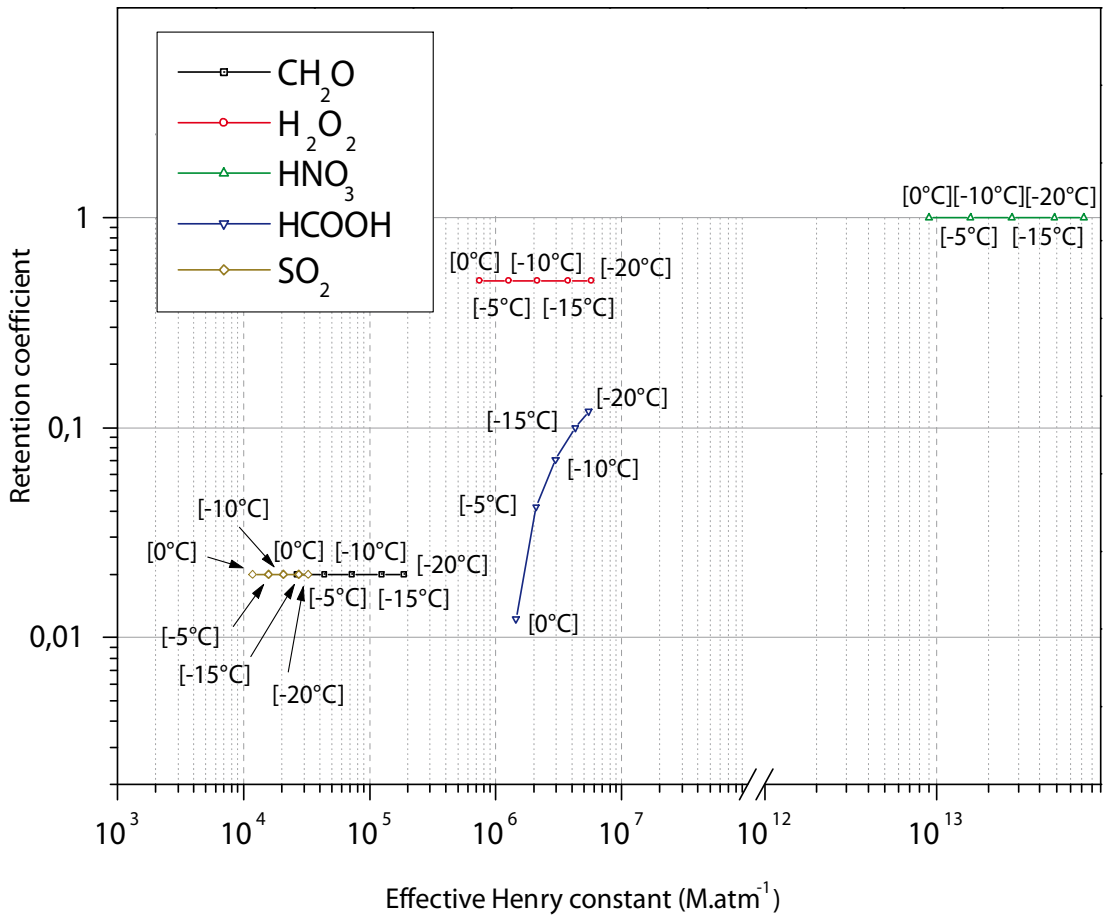


*Figure 2: Values of retention coefficients and effective Henry's law constants (pH is varying around a value of 5) for different temperatures (0, -5, -10, -15 and -20°C) and for several chemical species ($SO_2$, $CH_2O$, $H_2O_2$, $HNO_3$, $HCOOH$).*

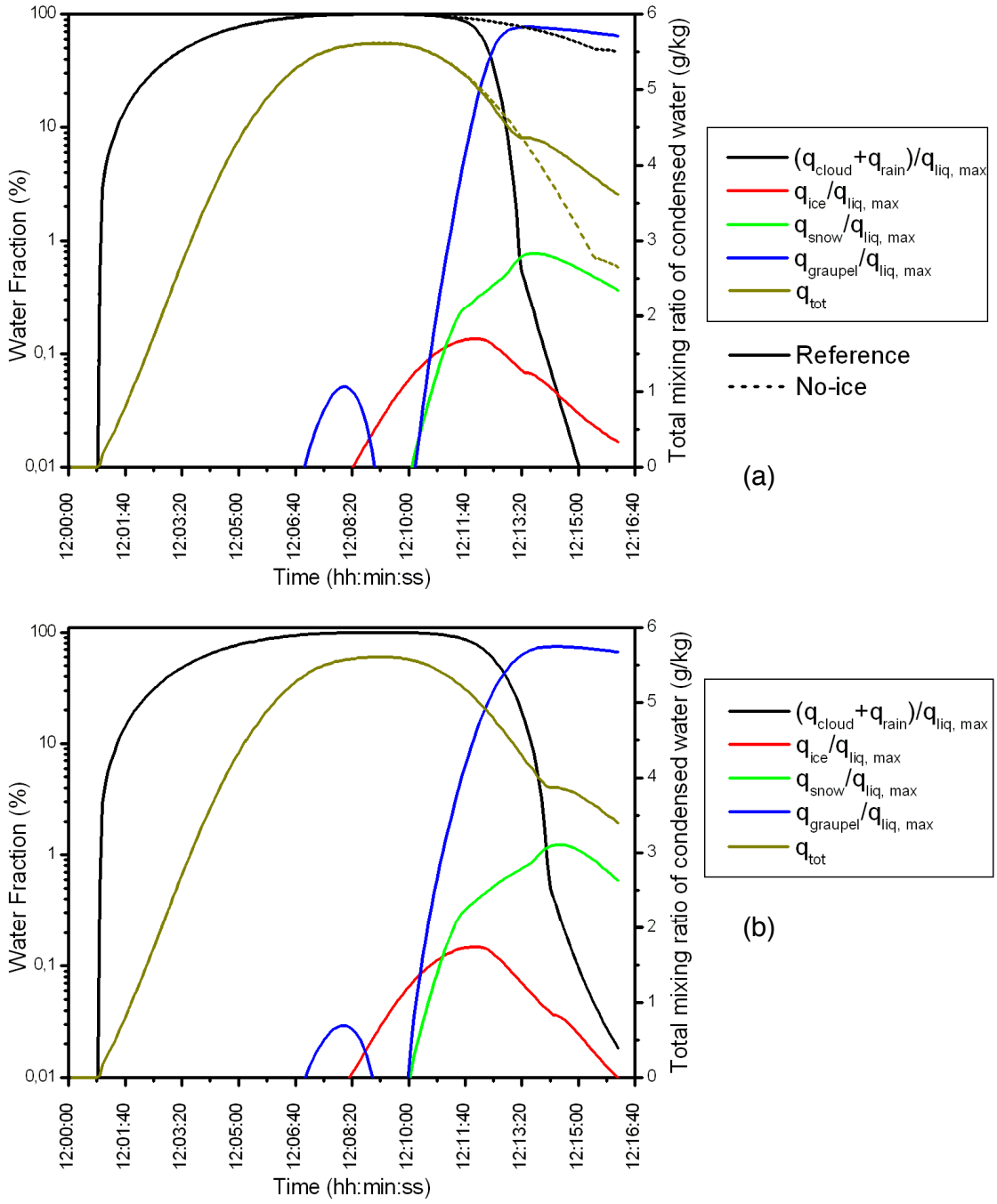


*Figure 3: a) Time evolution of the various hydrometeors fractions normalized by the maximum of the liquid water mixing ratio ($q_i$ = mixing ratio of the "i" hydrometeor). The total mixing ratio of condensed water expressed by the sum of* $q_{rain} + q_{cloud} + q_{ice} + q_{snow} + q_{graupel}$ *is indicated on the right Y-axis. Dotted lines represent the time evolution of the total mixing ratio and the water fraction when ice is neglected. b) Same as in Figure 3a but for spherical crystals.*

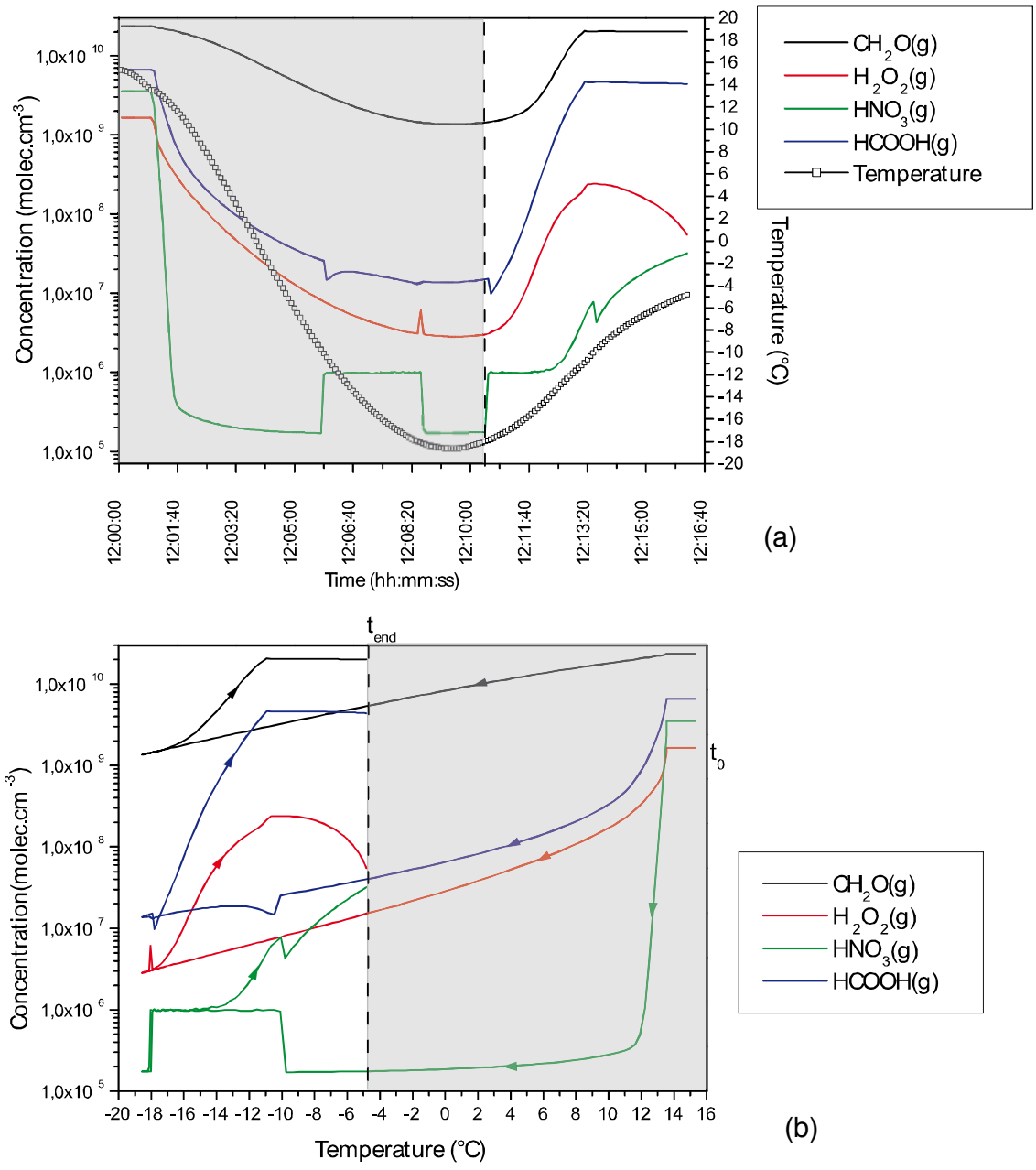


*Figure 4: a) Time evolution of gas phase concentrations in the reference case. Time evolution of the temperature is also drawn in black.*

*b) Evolution of gas phase concentration with temperature. The vertical dashed line materializes the separation between supercooled and ice processes.*

*The beginning and the end of the simulation are indicated with $t_0$ and $t_{end}$ respectively.*

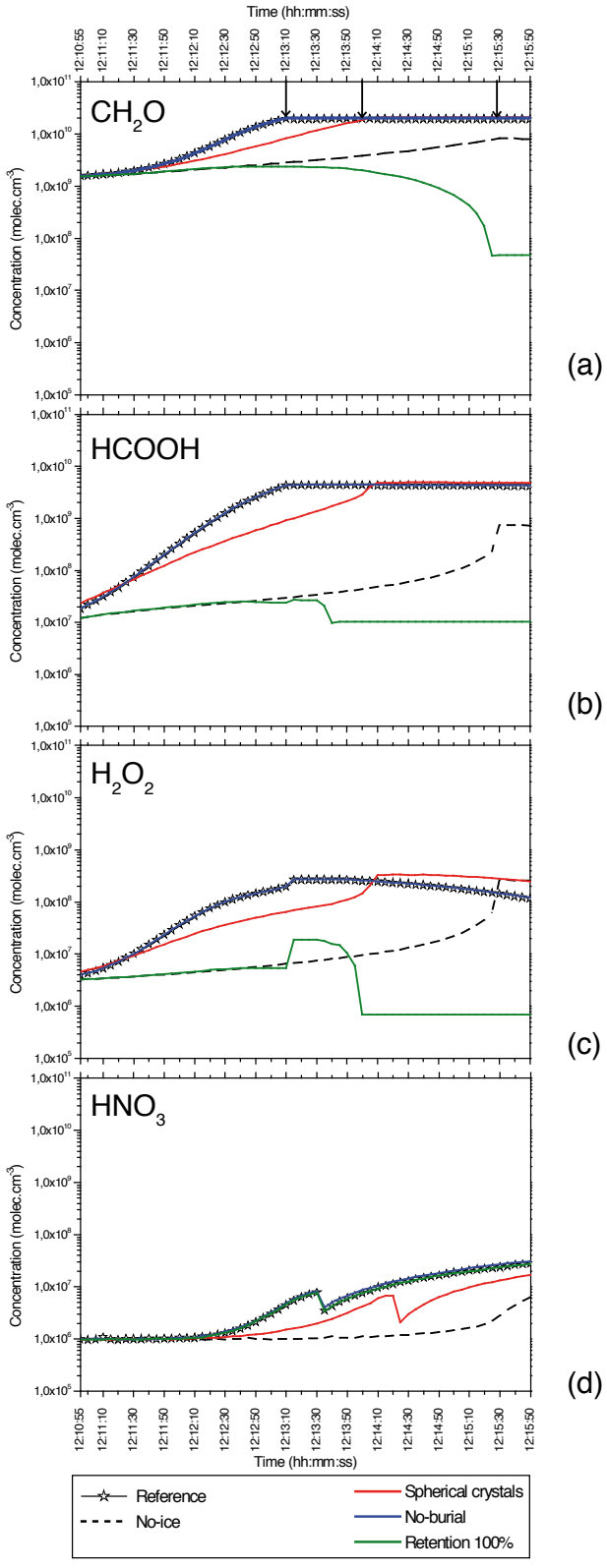


*Figure 5: Time evolution of gas concentrations for $CH_2O$, HCOOH, $H_2O_2$, $HNO_3$ for several simulations: the reference case (solid line), a case without ice, a case considering spherical crystals, a case neglecting burial, a case assuming full retention.*

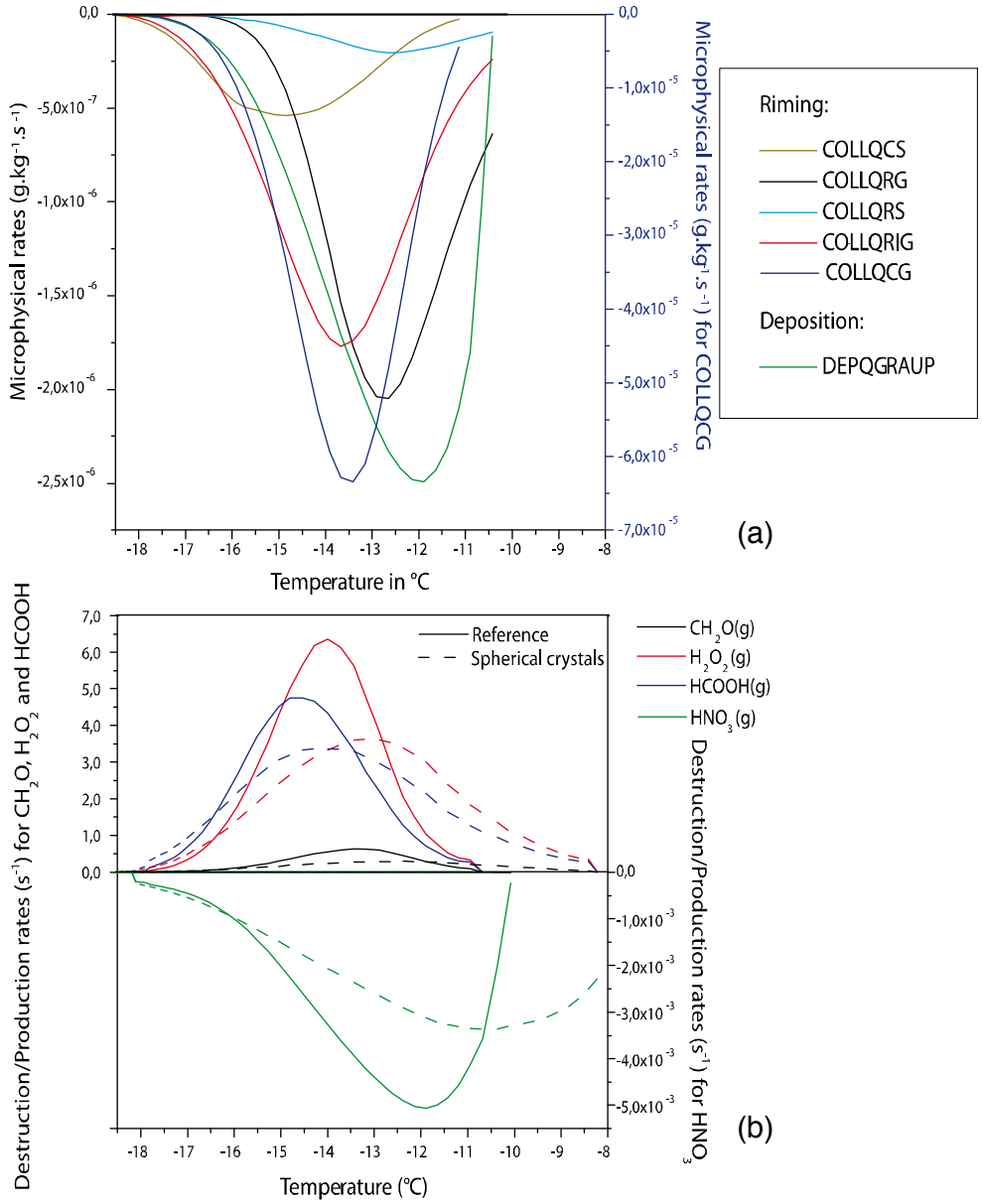


*Figure 6: a) Microphysical rates related to the riming, freezing and deposition processes versus temperature (note that collection growth of graupels by cloud droplets on graupel is one order of magnitude larger than the other rates on the right-hand side scale).*

*b) Evolution of gas species destruction or production rates* $\frac{1}{C_g}(\frac{\partial}{\partial t}C_g)_{RET\_BUR}$ *due to retention and burial effects as a function of temperature. Those rates correspond to the microphysical conversion rates shown in Figure 6a. Also, they are superimposed with the rates obtained for the simulation with spherical crystals (dashed lines).*

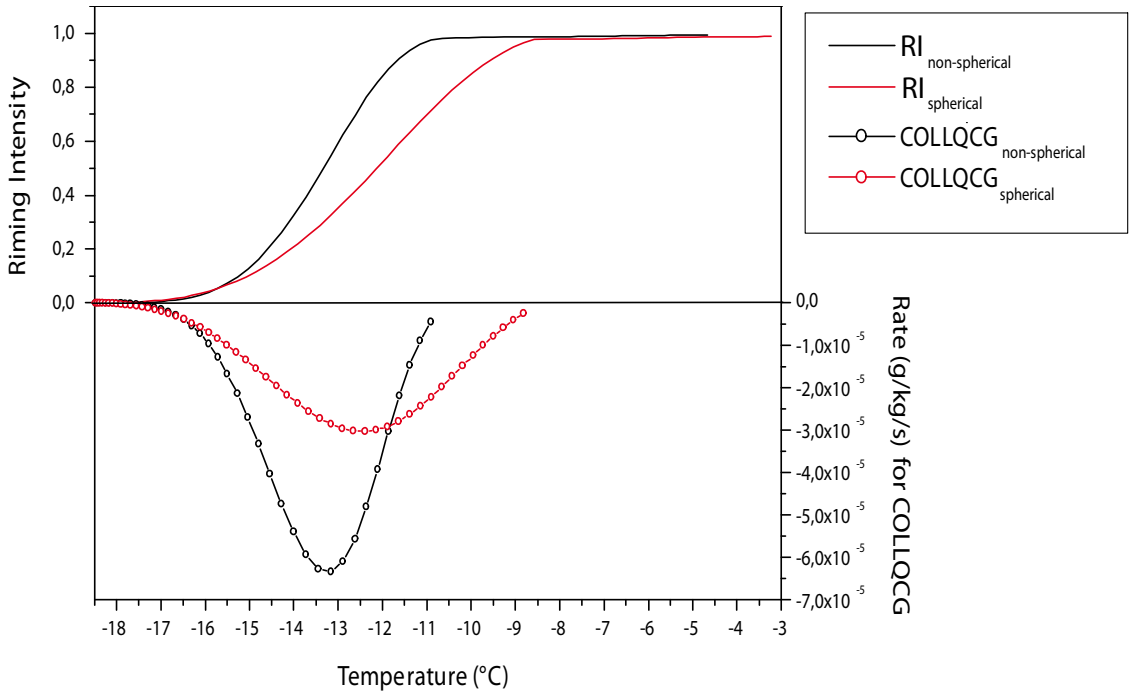


*Figure 7: Riming intensity for non-spherical (in black) and spherical (in red) cases versus temperature. The collection growth rate of graupel by cloud water on graupel COLLQCG is also drawn versus temperature (right-hand side scale).*

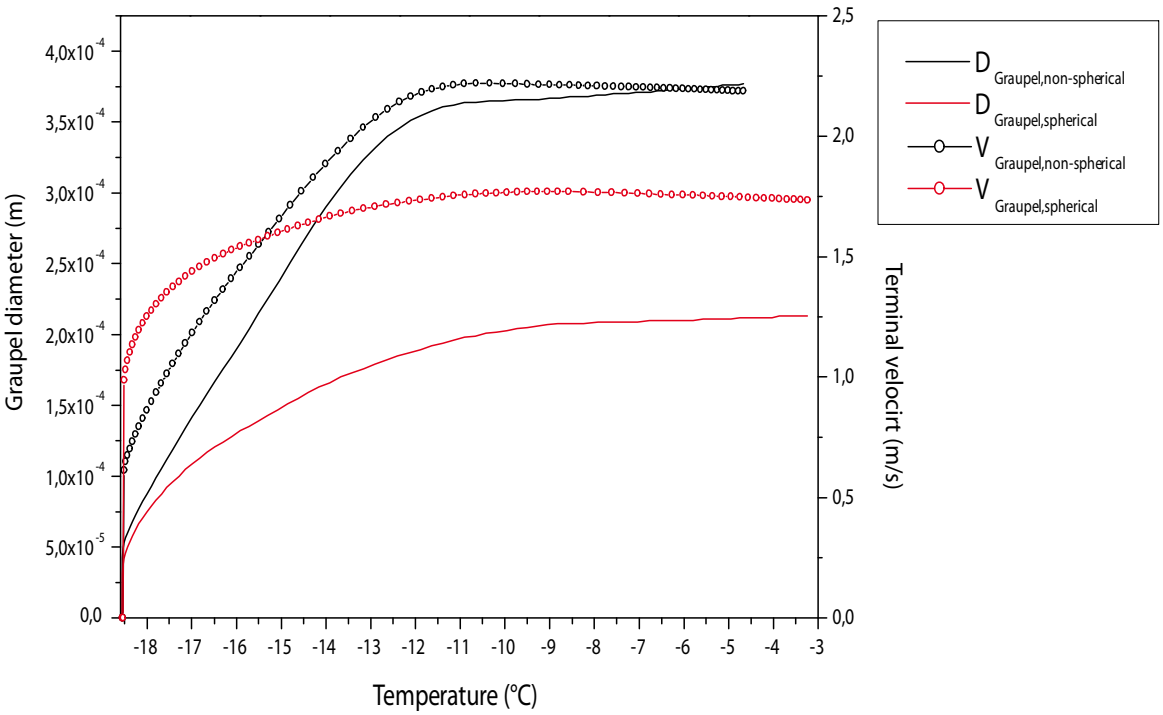


*Figure 8: Graupel diameter and terminal velocity for non-spherical (in black) and spherical (in red) cases versus temperature.*